Journal of Discrete Mathematics and Its Applications 8 (4) (2023) 187–200

Journal of Discrete Mathematics and Its Applications

Available Online at: http://jdma.sru.ac.ir

Shahid Rajaee Teacher Training University

Review Paper

Eyes on the cosmic web: A tribute to Ali Reza Ashrafi

Ottorino Ori[1,*], **Mihai Putz**[2,3]

[1]Actinium Chemical Research, Via Casilina 1626/A, 00133, Rome, Italy

[2]Laboratory of Computational and Structural Physical-Chemistry for Nanosciences and QSAR, Biology-Chemistry Department, Faculty of Chemistry, Biology, Geography, West University of Timisoara, Pestalozzi Str. No. 16A,RO-300115 Timisoara, Romania; mihai.putz@e-uvt.ro

[3]Scientific Laboratory of Renewable Energies-Photovoltaics, RD National Institute for Electrochemistry and Condensed Matter (INCEMC-Timisoara), Dr. Aurel Podeanu Str. No. 144, RO-300569 Timisoara, Romania; mvputz@yahoo.com

Academic Editor: Ivan Gutman

Abstract. This article delves into the subject of topological modeling and invariants in the study of the Cosmic Web (CW), which refers to the vast network of galaxies in the universe. The article explores the use of eccentric connectivity and other topological descriptors to classify various structures within the Cosmic Web, such as filaments, walls, and clusters. By analyzing graphs and lattices in detail, the study shows how topological invariants can be used to extract morphological information and categorize nodes based on their structural roles. Additionally, the article discusses the potential application of these methods in assigning galaxy populations across different structures within the Cosmic Web. This research offers valuable insights into the use of topological tools for comprehending the intricate and complex nature of the universe's large-scale galaxy distribution.

Keywords: power graph, characteristic polynomial, generelized coalescence
Mathematics Subject Classification (2010): 05C10, 05C25, 20*B*25.

*Corresponding author(*Emial address*:mailto:ottorino.ori@gmail.com)
Received 5 October 2023 ; Revised 20 October 2023 ; Accepted 5 November 2023
First Publish Date:1 December 2023

0.1 On Voronoi tessellations of the cosmic web and topological invariants

Back in 2017 during some talks with ALIREZA we had wandered about the usage of the eccentric connectivity index in the classification of the structures of the Cosmic Web (CW), the enormous graph of galaxies filling the universe. Almost by chance an example of an interesting usage of that invariant in classifying CW sub-structures (filaments, voids, clusters, etc). This discovery remained since then unexploited, and time to time - till Xmas last year - we have said"...we need to find an expert of cosmic topology to interact with or at least the access to a CW database for exercising on larger portions of the cosmic mesh and better check this resul". We're all missing him. Surely ALIREZA sees the sky secrets more closely now.

The use of topological tools such as graph topological invariants is used, since many years, for the classification of the various structures forming the Cosmic Web (CW). The observed large-scale distribution of galaxies presents in fact remarkable building elements, such as clusters of galaxies, filaments, sheets, walls and large voids. Original considerations on topological distance-based indices and the topological classifications of CW structural features are provided in the following paragraphs.

Topological modeling describes a physical system like a graph made by n-nodes and e-edges (only simple graphs are considered herewith), then takes a distance-based topological invariant ξ computed on G_n , treats ξ like a normal potential energy and finally minimizes it determining in this way the most stable configurations of the topological networks G_n. According to this basic topological approach:

Invariants like ξ naturally describe long-range interaction potentials, belonging to the class of all-neighbors-interactions.

A few descriptors ξ are considered in this note. Distance d_{ij} between two nodes i and j belonging to G_n equals to the number of bonds in the shortest path connecting that pair of vertices; $d_{ij} = k$, iff atom j appears in the k-coordination shell of i, and vice-versa; $d_{ij} = d_{ji}$ and $d_{ii} = 0$ for every pair i,j. Indicating with M the length of the longest distance - the integer M corresponds to graph diameter- and with b_{ik} the number of k-neighbors of atom i, the effects of the long-range connectivity properties of the whole lattice G_n on node i is summarized by topological invariant w_i:

$$w_i = \frac{1}{2}\sum_k k b_{ik},$$

with $k = 1,2,\ldots,M$, where $n = \sum_k b_{ik} + 1$. Node degree is b_{i_1}. Symbol $\underline{w}$ (or $\overline{w}$) indicates the smallest (the largest) w_i. Nodes with $w_i = \underline{w}$ (or $w_i = \overline{w}$) are the so-called minimal (or maximal) vertices of G_n. Integers b_{i_k} identify the Wiener-weights of vertex i (WW_i). The Wiener index W, the first topological descriptor applied to chemistry about seventy years ago, is obtained by:

$$W(n) = \frac{1}{2}\sum_{ij} d_{ij} = \sum_i w_i, \tag{1}$$

where $i, j = 1,2,\ldots,n$.

W provides the topological measure of the overall compactness of the system. For periodic lattices made by N unit cells U, index (1) presents a peculiar dependence from D the dimensionality system. With $D = 1$ it scales as N^3, whereas the general case of a lattice made by N^D unit cells shows a typical $W(N) \approx N^{2D+1}$ dependence in the large N limit. For *D=2* the lattice has $N_x \times N_y = N^2$ unit cells. If each unit cell contains α nodes, the total number of nodes in the graph is $n = \alpha N^D$ thus one has $W(n) \cong n^{2+1/D}$ dependence conjectured valid so far for all lattices (see footnote) with the really intriguing $\approx D^{-1}$ "vanishing" of the influence of the space dimensions for spaces with high D.

When graphs G_n^* with closed boundaries are taken into consideration, the compression factor of the Wiener index $f_W = W^*/W$ respects the following inequality in the limit for large n:

$$f_W \leq \frac{3}{4}. \tag{2}$$

The universal behavior (2) is conjectured to be valid for any pair G_n andG_n^* of open/closed graphs, irrespectively from graph complexity or dimensionality. In particular the upper limit $f_W = 0.75$ strictly holds for (*i*) any kind of *D=1* lattices and (*ii*) any D-dimensional cubic lattices. No other general properties regarding f_W have been derived so far to confirm or dismantle the conjecture (2).

Going back to topological modeling (TM) we introduce here the first rule: a higher reactivity is locally assigned to nodes with maximal w_i. This is our first approximation. The following lattice descriptors:

$$\rho = \frac{W}{n\underline{w}}, \tag{3}$$

$$\rho^E = \frac{\overline{w}}{\underline{w}}, \tag{4}$$

respect, by definition, the inequalities $\rho \geq 1$ and $\rho^E \geq 1$; ρ measures the ability of the lattice to self-arrange around the minimal vertices, which are the most efficient nodes in term of compactness, maximizing in such a way the overall compactness. For this reason ρ has been called topological efficiency index [2] and, more recently, it is also used for ranking the topological roundness of the structure. For example, ideal (infinite) graphene or cubic tori have $\rho = \rho^E = 1$. Playing an analogous role,ρ^E is named extreme topological efficiency index.

So infinite cubic lattices or infinite graphene layers, together with icosahedral C_{60} molecules, are examples of perfectly spherical structures (topologically speaking), good to know.

Higher stability is globally assigned to structures with maximal topological roundness. Thus systems tend to evolve to minimize ρ or ρ^E and this is the second approximation.

The eccentric connectivity ξ_i of the node i and of the graph (G) are defined as:

$$\xi_i = b_{i_1}\varepsilon_i, \tag{5}$$

$$\xi(G) = \sum_i \xi_i, \tag{6}$$

in which the topological eccentricity $\varepsilon_i = max\{d_{ij}\}$ represents the maximum distance between i and the remaining nodes. Invariant (5) is used herewith for ranking the topological localization of node i according to the following criterion.

Nodes belonging to filaments, wall, clusters show different values of their eccentric connectivity. And this is the third approximation.

It is worth mentioning that the three approximations exposed above are at the heart of topological modeling methods, and they hold only when similar topological networks are compared.

1 SUMMARY OF RESULTS

Reference lattice H

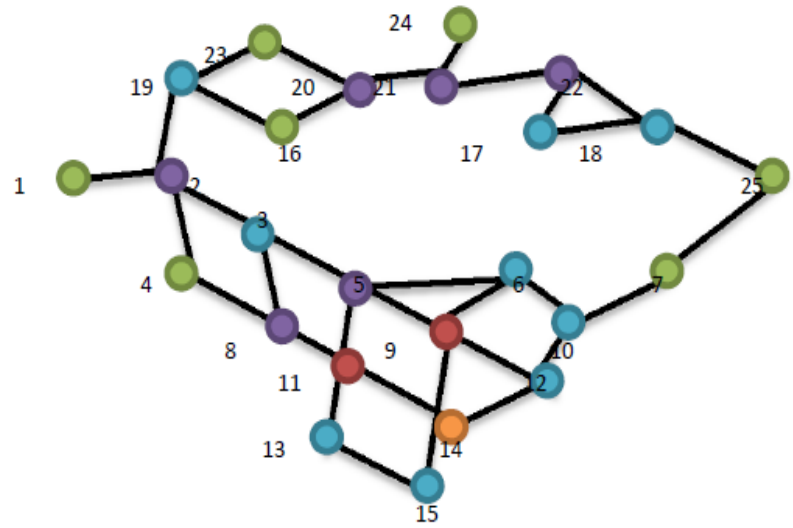

Figure 1. Graph H.

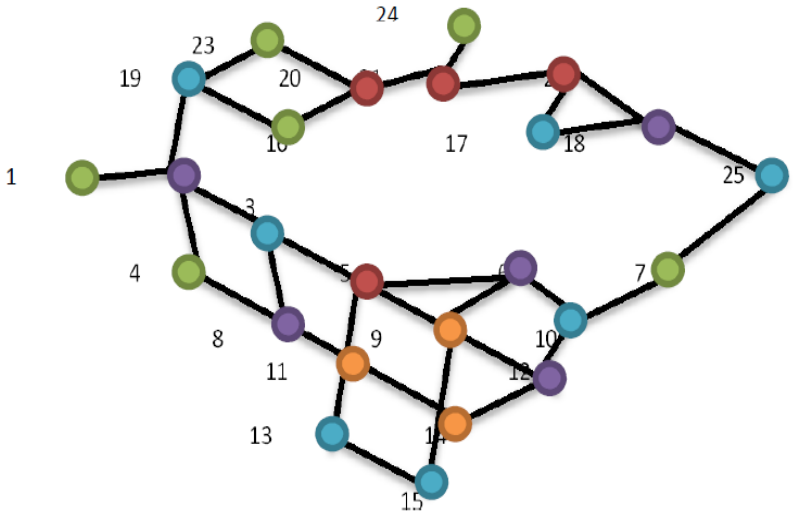

Figure 2. Graph H^C, nodes 1 and 25 are bonded.

Graph	n	W	M	Bonds	$\underline{w}$	$\overline{w}$	ρ	ρ^E	$\xi(G)$
H	25	1211	9	34	39	64.5	1.242	1.654	500
H^C	25	1136	9	35	35	64	1.298	1.829	495

Table 1. Topological invariants for H and H^C.

The graph H with 25 nodes is used here as reference system. This lattice is built by assembly nodes with maximum degree 4, see the unit cell provided in Figure 1. This lattice is supposed to grow by 1-25 joints.

In the open H lattice all atoms are non-equivalent having different sets $\{b_{ik}\}$; in such a lattice minimal (maximal) vertices are nodes 5 and 24 respectively. The minimal string $\{b_{k5}\}$, $k = \varepsilon_i = 7$ results as follows: $\{b_{k5}\} = \{4,6,5,3,2,3,1\}$. with a peak of 6 neighbors in the $k = 2$ shell population (Table 3). The plot of WW shows the following characteristics:

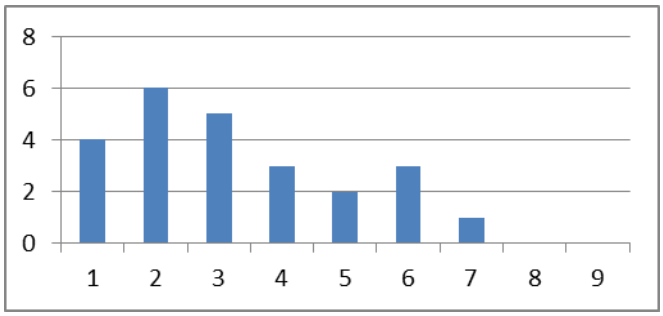

Figure 3. Above shape may be compared with a similar curve for minimal nodes in pristine honeycomb lattices, starting with an obvious $b_1 = 3$.

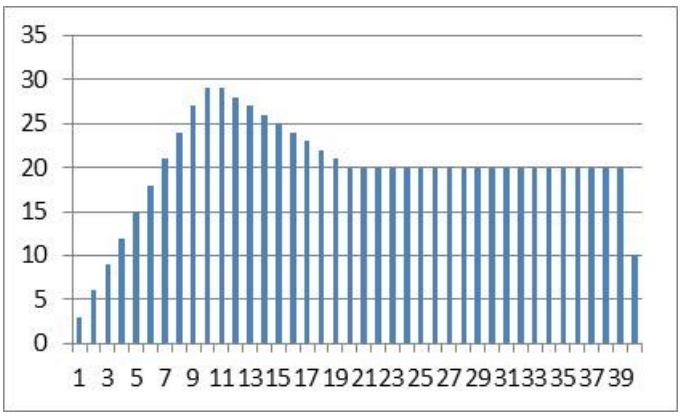

Figure 4. The above b_k histogram represents the topological fingerprint of the ideal graphene lattice without defects.

The diagram below represents instead the population for the maximal node $i = 24$. A low coordination degree ($b_1 = 1$) and highest eccentricity $\varepsilon_i = M$ are typical signatures of this kind of very reactive (unstable) nodes.

In Figure 1 various (arbitrary) colors group nodes sorted by the values of their invariant (5). The "green" set groups nodes with the lowest eccentric connectivity values ξ_i mostly have similar structural role appearing to cover filaments. Similarly, blue ones seem to define boundaries of ticker regions, while the red circles select embedded nodes.

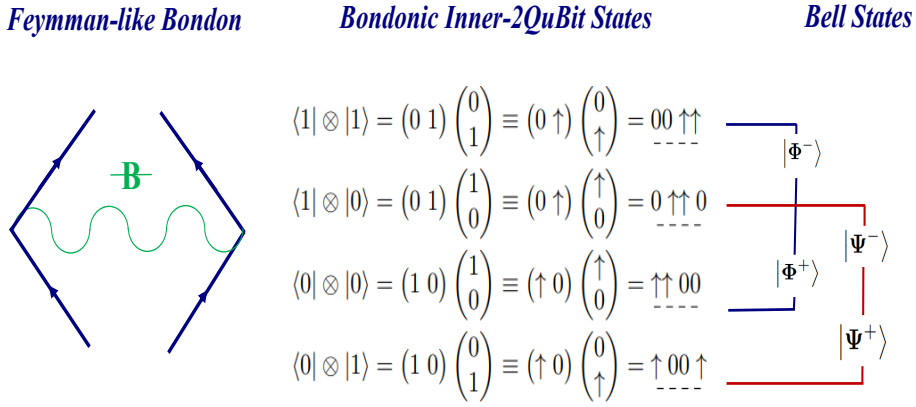

The ability of the eccentric connectivity ξ_i to provide structural indications may be not totally unexpected since this invariant (5) carries topological information, both local (the degree) and long-distance (maximum coordination shell), that characterizes nodes in the network graph.

2 Lattices with periodic condition H^C

Imagine to close H graph by "adding" an extra-bond between nodes 1 and 25 of Figure 1. The resulting network constitutes in fact a kind of loop; this new topology H^C influence the structural role of some of its nodes, namely the bridging vertex 25, see Figure 2. Other sets of nodes still keep an apparent structural coherence, for example vertices 21-17-22 still form a filament and 11-9 identify the central nodes.

Nodes composing H^C network are again non-equivalent showing different $\{b_{ik}\}$ sets; minimal (maximal) vertices are nodes 2 and 15 respectively, whose string $\{b_{k5}\}$ are provided in Table 4. It is worth mentioning that topological invariants in Table 1 look quite similar just because these graphs with $N = 1$, $n = 25$ are still quite small. By adding more unit cells the two lattices behave quite diversely in fact. When $N = 25$ unit cells are assembled to form a linear lattice $D = 1$ by joining nodes 1 and 25, lattices with $n = 625$ and the following invariants in Table 1 are computed. The expected relations in the large-n limit like $M^C \approx M/2$, $W \approx 1.33W^C$ and $W \approx \rho W^C$ are realized. The last one, that involves ρ, reflects another conjecture:

$$f_W = \rho^{-1}, \tag{7}$$

Graph	n	W	M	Bonds	$\underline{w}$	$\overline{w}$	ρ	ρ^E	$\xi(G)$
H	625	1325527	5199	874	15819	31312.5	1.341	1.979	262122
H^C	625	1000362	5102	875	15815	16436.5	1.012	1.031	176900

Table 2. Topological invariants for H and H^C.

for compression factor f_W valid for all graphs so far.

Minimal (maximal) nodes in H^C (namely 2 and 15) vary from the previous open case with the relative WW showing however the usual differences in shapes being one more compact (shoulder-like) and the other more spread along the shells, respectively $b_{k2} = \{4,5,6,7,2\}$, $k = 1,2,..5$ and $b_{k15} = \{2,3,4,3,2,3,4,2,1\}$, $k = 1,2,\ldots,M$, with the same shapes reported for the open graph H in previous histograms.

3 Cosmic Web networks V_1 and V_2

In [22] and related studies, the topology of the Megaparsec Cosmic Web (CW) is approached in terms of scale-dependent Betti numbers, a scaling technique to extract the topological information contained in or influencing in the cosmic mass distribution. Authors recognize that Betti numbers "do not fully quantify topology" basing the analysis for the discrete galaxy distribution on the alpha shapes of the network by creating ordered sequences of nested subsets of the Delaunay tessellation with scaling filtration parameter α. The method is recursively applied first to the heuristic study of Voronoi clustering modeling the morphological patterns (i.e. clusters, filaments, or sheets) in the CW.

The alpha shapes method suffers, like most of the parametrized scaling technique on a graph, of a certain level of "arbitrariness", causing the resulting CW morphology to be critically dependent form the filtration parameter α and the selected filtration sequence. Here the aim of the current section consists therefore in applying the topological invariants (1) to (6) to the same pair of Voronoi reference structures given in Figure 2 of article [22], see Figure 3 below.

In particular we will show how the eccentric connectivity computed for each node (5) conveys a certain level of information on CW morphology without using scale-parameters like the Voronoi disk radius. This method aims in fact to extract the "genuine" topological features embedded in the galaxy CW mesh just studying the long-distance properties arising from the connectivity of the mesh, without extra-parameters, supporting in such a specific way all types of topological investigation. We investigate the two lattices presented in Figure 3 where small-radius and large-radius Voronoi tessellations V_1 and V_2 are on left and right, respectively.

The delaunay simplices, arising from the dual representation of the union of Voronoi disks, are also shown as by the Voronoi polygons in Figure 3 in which the classification of node resulting from their eccentric connectivity values ξ_i is represented by colored circles. This topological ranking looks quite interesting since nodes placed in given sub-structures

H node	WW	b_{i_1}	ϵ_i	ξ_i	w_i
v_1	1 3 4 4 5 4 3	1	7	7	52,5
v_{24}	1 2 4 2 2 4 4 3 2	1	9	9	64,5
v_7	2 3 5 4 5 5	2	6	12	47
v_4	2 4 5 5 2 3 3	2	7	14	47
v_{16}	2 3 5 4 4 5 1	2	7	14	48
v_{23}	2 3 5 4 4 5 1	2	7	14	48
v_{25}	2 3 3 5 5 4 2	2	7	14	50
v_{17}	2 2 3 3 3 4 5 2	2	8	16	58,5
v_{10}	3 4 4 5 4 4	3	6	18	43,5
v_{13}	2 3 5 2 3 3 2 3 1	2	9	18	55,5
v_{15}	2 3 4 3 2 3 4 2 1	2	9	18	56,5
v_{19}	3 4 3 5 6 3	3	6	18	44
v_3	3 6 6 3 2 3 1	3	7	21	40
v_6	3 5 5 4 4 2 1	3	7	21	41,5
v_{12}	3 5 4 3 4 3 2	3	7	21	44,5
v_{18}	3 2 3 4 4 4 4	3	7	21	52
v_2	4 4 4 5 4 3	4	6	24	41
v_8	3 4 6 3 2 2 3 1	3	8	24	46
v_{20}	3 3 3 4 3 4 3 1	3	8	24	51
v_{21}	3 4 2 2 4 4 3 2	3	8	24	53
v_{22}	3 3 3 2 3 6 3 1	3	8	24	53
v_5	4 6 5 3 2 3 1	4	7	28	39
v_9	4 4 4 4 3 3 1 1	4	8	32	44
v_{11}	4 6 2 3 3 2 3 1	4	8	32	45

Table 3. Topological eccentric connectivity for H sorted by ξ_i.

H^C node	WW	b_{i_1}	ϵ_i	ξ_i	w_i
v_{24}	1 2 4 2 3 3 4 3 2	1	9	9	64
v_7	2 4 6 6 6	2	5	10	41
v_1	2 5 7 6 3 1	2	6	12	39
v_4	2 4 6 7 4 1	2	6	12	41
v_{16}	2 3 5 5 4 4 1	2	7	14	47
v_{23}	2 3 5 5 4 4 1	2	7	14	47
v_{17}	2 2 4 4 5 4 2 1	2	8	16	52.5
v_3	3 6 7 4 3 1	3	6	18	36.5
v_{10}	3 4 5 5 3 4	3	6	18	42.5
v_{13}	2 3 5 2 3 3 2 3 1	2	9	18	55.5
v_{15}	2 3 4 3 2 3 4 2 1	2	9	18	56.5
v_{19}	3 4 4 7 5 1	3	6	18	41
v_{25}	3 4 6 8 2 1	3	6	18	38.5
v_2	4 5 6 7 2	4	5	20	35
v_6	3 5 5 4 4 2 1	3	7	21	41.5
v_8	3 4 6 4 3 3 1	3	7	21	42.5
v_{12}	3 5 4 4 3 3 2	3	7	21	44
v_{18}	3 3 4 7 4 2 1	3	7	21	44
v_{20}	3 3 3 4 3 4 3 1	3	8	24	51
v_{21}	3 4 2 3 3 4 3 2	3	8	24	52.5
v_{22}	3 3 4 3 4 4 2 1	3	8	24	49.5
v_5	4 6 5 3 2 3 1	4	7	28	39
v_9	4 4 4 4 3 3 1 1	4	8	32	44
v_{11}	4 6 2 3 3 2 3 1	4	8	32	45

Table 4. Topological eccentric connectivity for H^C sorted by ξ_i.

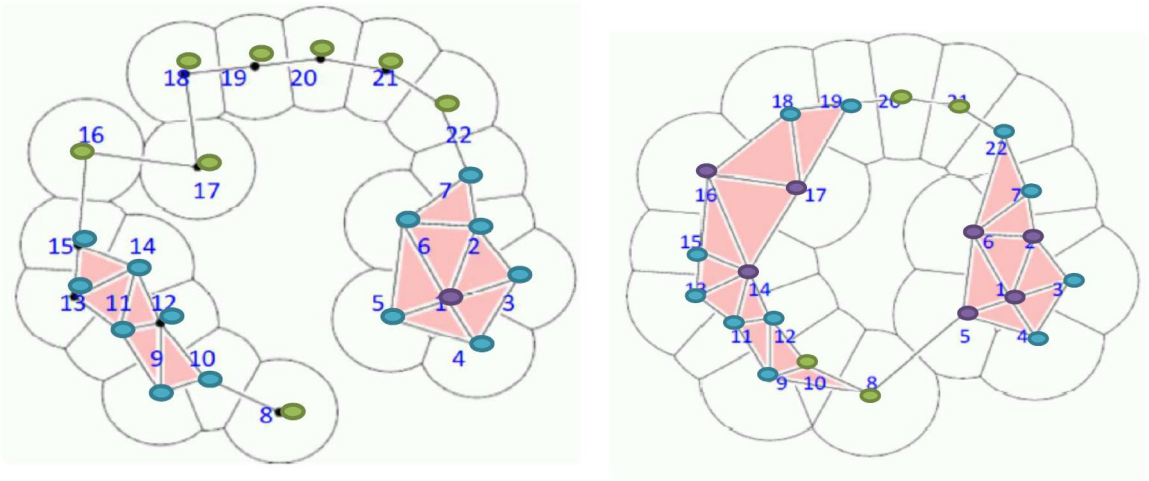

Figure 5. (left): graph V_1, the sample cluster of galaxies whose graph depends from small Voronoi radius. (right): similar representation for graph V_2 based on larger small Voronoi disks. Both graphs show a good fit between the set of ordered values of ξ_i (represented by colors) and their morphological role. Green indicate filament nodes, blue the wall, purple the cluster ones. In open graph like V_1 topological ξ_i -sorting of nodes appears to work more efficiently.

show similar values. The galactic cluster in Figure 3 top corresponds, for small value of Voronoi radius, to an open galactic structure, in which green nodes (ranked by invariant ξ_i of Eq.(5)) occupy filaments, the blue ones look more localized on wall surfaces, whereas the purple vertex is deeper embedded in the structure.

What is quite interesting is that V_1 nodes may be ordered by their eccentric connectivity ξ_i and grouped to respect their morphological character, see Table 5 and Figure 3 top. For example, it is evident in Table 5 that wall nodes (blue) come after the green one representing the 8 filament galaxies $v_8v_{19}v_{18}v_{20}v_{17}v_{21}v_{16}v_{22}$. In the same way, the core galaxy v_1 arrives, in this ξ_i classifications, after all the wall blue nodes. This is quite an encouraging result -although needing further investigations- based on a single topological descriptor working on the topology of the CW graph.

Similar morphology-related ranking is obtained when the topological invariants ξ_i are computed for galaxies in V_2 graph, see Figure 3 bottom and Table 6. In open graph like V_1 the proposed method for distinguishing nodes appears to work better. Future extended investigations are needed.

We also like to evidence that, according to their w_i numbers in Table 5, node v_8 and v_5 are among the less stable vertices of graph V_1 (in effect V_8 is the maximal node of that graph) and then are nodes that tend to reach more-stable configuration in the network by changing their connectivity. Intriguingly enough, they are in fact the same 2 nodes getting bridged by a new bond during the passage to increased-disk-radius Voronoi graph V_2. In Table 7 this evolution path eg $V_1 \to V_2$ evolution trend, is also confirmed by the other topological indicators being V_2 more compact (having lower Wiener and eccentric connectivity indices) and topologically more round and efficient (having lower ρ and ρ^E indices). Table 6 moreover points out that

V_1 node	WW	b_{i_1}	ε_i	ξ_i	w_i
v_8	1 2 2 2 1 1 1 1 1 1 1 2 3 1	1	15	15	85
v_{19}	2 2 2 2 4 5 3 1	2	8	16	49,5
v_{18}	2 2 2 3 3 4 4 1	2	8	16	49,5
v_{20}	2 2 2 3 4 3 2 2 1	2	9	18	50,5
v_{17}	2 2 3 3 3 2 2 3 1	2	9	18	50,5
v_{21}	2 2 3 4 2 1 2 2 2 1	2	10	20	52,5
v_{16}	2 3 3 3 2 1 1 2 3 1	2	10	20	52,5
v_{22}	2 3 4 2 1 1 1 2 2 2 1	2	11	22	55,5
v_{15}	3 3 3 2 1 1 1 1 2 3 1	3	11	33	55,5
v_7	3 4 2 1 1 1 1 1 2 2 2 1	3	12	36	59,5
v_{13}	3 3 2 2 1 1 1 1 1 2 3 1	3	12	36	61,5
v_3	3 3 1 1 1 1 1 1 1 1 2 2 2 1	3	14	42	73,5
v_5	3 3 1 1 1 1 1 1 1 1 2 2 2 1	3	14	42	73,5
v_9	3 3 1 1 1 1 1 1 1 1 1 2 3 1	3	14	42	74,5
v_{10}	3 2 2 1 1 1 1 1 1 1 1 2 3 1	3	14	42	75
v_4	3 2 1 1 1 1 1 1 1 1 1 2 2 2 1	3	15	45	81,5
v_{14}	4 3 2 1 1 1 1 1 1 2 3 1	4	12	48	60
v_2	4 3 1 1 1 1 1 1 1 2 2 2 1	4	13	52	65,5
v_6	4 3 1 1 1 1 1 1 1 2 2 2 1	4	13	52	65,5
v_{12}	4 3 1 1 1 1 1 1 1 1 2 3 1	4	13	52	66,5
v_{11}	4 2 2 1 1 1 1 1 1 1 2 3 1	4	13	52	67
v_1	5 1 1 1 1 1 1 1 1 1 2 2 2 1	5	14	70	72,5

Table 5. Topological descriptors for V_1 sorted by ξ_i.

V_2 node	WW	b_{i1}	ε_i	ξ_i	w_i
v_{20}	2 3 4 7 5	2	5	10	36,5
v_{21}	2 3 5 5 6	2	5	10	36,5
v_{10}	3 3 7 6 2	3	5	15	32
v_8	3 5 6 4 3	3	5	15	31
v_{13}	3 4 4 2 4 4	3	6	18	37,5
v_{19}	3 3 5 4 4 2	3	6	18	36
v_{22}	3 4 4 4 4 2	3	6	18	35,5
v_{11}	4 5 3 4 5	4	5	20	32
v_{12}	4 5 3 4 5	4	5	20	32
v_9	4 3 6 6 2	4	5	20	31
v_{15}	3 4 3 2 2 4 3	3	7	21	41,5
v_{18}	3 3 4 3 3 3 2	3	7	21	40
v_3	3 3 2 3 3 3 4	3	7	21	44
v_4	3 3 4 3 3 4 1	3	7	21	39,5
v_7	3 4 3 3 4 3 1	3	7	21	38,5
v_5	4 6 3 3 4 1	4	6	24	31,5
v_{16}	4 4 3 2 2 4 2	4	7	28	38,5
v_{17}	4 5 3 2 3 3 1	4	7	28	35,5
v_2	4 3 2 3 3 4 2	4	7	28	40,5
v_1	5 3 3 3 3 4	5	6	30	35,5
v_6	5 4 3 3 4 2	5	6	30	33
v_{14}	6 4 2 2 4 3	6	6	36	33

Table 6. Topological descriptors for V_2 sorted by ξ_i.

nodes $v_3v_{15}v_{18}v_2$ are, due to their high w_i values, the most reactive sites in the structure V_2 and are therefore keen to undertake connectivity changes letting V_2 to evolve toward more efficient graphs V_3. Future work is required to asses this method.

The main outcome of current preliminary study performed on the two very simple galaxy clusters V_1 and V_2 described above consisted in

Showing the ability of topological invariants to extract morphological information of the nodes in a CW graph. In particular node eccentric connectivity ξ_i appear capable to classify nodes on the basis of their structural role (filaments, walls, and clusters); w_i ranks stability of the nodes of the galactic mesh.

Similar analysis are applied in [19] to the study of the cosmic web, the large scale galaxy distribution, measuring topological quantities on a network built from the Cosmological Evo-

Graph	n	W	M	Bonds	w	w_{av}	ρ	ρ^E	$\xi(G)$
V1	22	1397	15	32	49.5	85	1.283	1.717	798
V2	22	791	7	39	31	44	1.160	1.419	473

Table 7. Topological invariants for V_1 and V_2.

lution Survey (COSMOS). These studies may be reinforced by adding topological invariants ξ_i and w_i to better allocate galaxy populations over the various CW structures (filaments, walls, and clusters).

3.1 Mark Table and Markaracter Table

The notion of the table of marks of a finite group was first introduced by William Burnside, one of the pioneers of finite groups, in the second edition of his classical book, see [2]. Shinsaku Fujita on the other hand, introduced the term "markaracter" to describe a unified framework for understanding marks of permutation representations and characters of linear representations on a common basis. The markaracter table, therefore, is a table that contains information about the marks and characters of a finite group, presented consistentently.

In contrast, the table of marks, which was introduced by Burnside, only describes the marks of a finite group's permutation representations. Fujita's markaracter table extends Burnside's table of marks to include both permutation and linear representations of a finite group. This unified framework provides a more comprehensive understanding of the structure of finite groups and their representations, see [4,5,7–15,17].

The table of marks of a finite group is a compact way to describe the subgroup lattice of a finite group G. It characterizes the permutation representations of G by certain numbers of fixed points and provides a detailed partially ordered set of all conjugacy classes of subgroups of G. The table is constructed by considering the set of all subgroups of G, denoted as $\Gamma_G = \{U : U \leq G\}$, and the G-action on Γ_G by conjugation. The G-orbits of subgroups in Γ_G form a partially ordered set, where the incidence relation is given by $[U] \leq [V]$ if $U \leq V^g$ for some $g \in G$.

Let $G_1(=1), G_2, \cdots, G_r(=G)$ be representatives of the conjugacy classes of subgroups of G. Then $\Gamma_G/G = \{[G_i], i = 1,2,\cdots,r\}$. For each subgroup $U \leq G$ the group G acts transitively on the set $U/G = \{Ug : g \in G\}$ of right cosets of U in G. Conversely every transitive G-set X is isomorphic to a G-set U/G where U is a point stabilizer of X in G. For every $g \in G$ the G-set U^g/G is isomorphic to U/G. Thus every transitive G-set is isomorphic to G_i/G for some $i \leq r$.

Definition 1. Let G be a finite group, X be a G-set and $U \leq G$. The mark $\beta_X(U)$ of U on X is define as

$$\beta_X(U) = |Fix_X(U)|,$$

where $Fix_X(U) = \{x \in X : x.u = x, \forall u \in U\}$ is the set of fixed points of the subgroup U in the action of G on X.

The table of marks $M(G)$ is a square matrix

$$M(G) = (\beta_{G_j/G}(G_i))_{j,i},$$

where G_i and G_j run through of non-conjugated subgroups of G.

The markaracter table of G is obtained by selecting rows and columns from $M(G)$ corresponding to cyclic subgroups of G. Shinsaku Fujita introduced the term "markaracter" in some of his seminal papers [1, 15, 17, 18, 20, 21] to refer to marks for permutation representations and characters for linear representations in a common basis.

The paper [1] describes a straightforward computational method for calculating the markaracter tables of finite groups. With this method, the authors were able to compute the markaracter table of a dihedral group of order $2n$, as well as several abelian groups. The paper also includes a GAP program that is effective for calculating markaracter tables of groups with order $d \leq 10000$. Using this program, the markaracter table of the I_h point group symmetry was calculated.

Let G be a permutation group. The cycle index of G acting on X is the polynomial $Z(G, X)$ over Q in the indeterminates $x_1, x_2, \cdots x_t$, $t = |X|$, defined by

$$Z(G, X) = \frac{1}{|G|} \sum_{g \in G} \Pi_{i=1}^{t} x_i^{c_i(p)},$$

in which $(c_1(p), \cdots, c_t(p))$ is the cycle type of the permutation $p \in G$. All elements of a conjugacy class have the same cycle type, so the cycle index can be rephrased in the following way:

$$Z(G, X) = \frac{1}{|G|} |C| \sum_{c \in C} \Pi_{i=1}^{t} x_i^{c_i(gc)},$$

where C is the set of all conjugacy classes of G with representatives $gc \in C$.

In papers [20,21], Ashrafi et al. calculated the markaracter table of generalized quaternion groups and finite groups of order pqr, where p, q, and r are prime numbers and $p \geq q \geq r$. This work demonstrated Ashrafi's expertise in the area of group theory and his ability to make significant contributions to the field. His collaborations with other researchers, as evidenced by these papers, also highlighted his commitment to working with others and sharing knowledge.

Fullerenes are a class of carbon molecules that have a unique spherical structure, and the fullerene C_{60} is a particularly well-known example. The symmetry group of C_{60} is a group of transformations that preserve the structure of the molecule, such as rotations and reflections.

In [16, 18] they computed the $USCI$ table and cycle index of some classes of fullerene graphs. The concept of unit subduces cycle indices (USCIs) is a mathematical tool used in the study of symmetry groups and their actions on sets of objects. USCIs are polynomial expressions that encode the symmetry properties of a finite group and are used to calculate the number of fixed points and cycles under group actions. More specifically, USCIs are

derived from the cycle index polynomial of a finite group, which is a polynomial expression that encodes the group's permutation action on a set of labeled objects.

The cycle index polynomial can be used to count the number of permutations that leave a set of objects invariant, as well as the number of permutations that have a given cycle structure.

The USCIs are obtained by taking the unit subductions of the cycle index polynomial, which involves substituting certain variables in the cycle index polynomial with unity. The resulting polynomial expresses the number of fixed points and cycles of the group action on subsets of the original set of objects.

The concept of USCIs is closely related to the Polya enumeration theorem, which is a mathematical theorem used to count the number of orbits of a finite group on a set of objects. The USCIs can be used in conjunction with the Polya enumeration theorem to systematically count the number of isomers of chemical compounds based on their underlying symmetry groups. The use of USCIs has important applications in the fields of chemistry and materials science, as it provides a systematic and efficient way to predict and enumerate the structural isomers of compounds and materials based on their underlying symmetry groups.

The main content of the paper [3] is an analysis of the cycle index of the symmetry group of C_{60}. The cycle index is a mathematical tool used to describe the cycle structure of a permutation group, which is a group of transformations that rearrange a set of objects.

In the paper, Fripertinger derives an explicit formula for the cycle index of the symmetry group of C_{60}, which allows for a detailed analysis of the group's cycle structure. This analysis provides insights into the geometric and chemical properties of the molecule, such as its bond lengths, bond angles, and electronic structure.

The paper also includes several examples and applications of the cycle index formula, demonstrating its usefulness for predicting and analyzing various properties of C_{60} and related fullerene structures. Overall, the paper represents an important contribution to the field of mathematical chemistry and demonstrates the power of group theory and other mathematical tools for understanding the properties of complex molecular structures. Finally, in [18] the authors generalized Fripertinger's method to compute the three-dimensional Polya cycle indices for the natural actions of the symmetry group on the set of vertices, edges, and faces of the small fullerene C_{24} and the big fullerene C_{150}.

References

[1] A. R. Ashrafi, M. Ghorbani, A note on markaracter tables of finite groups, *MATCH Commun. Math. Comput. Chem.* **59** (2008) 595–603.

[2] W. Burnside, *Theory of Groups of Finite Order*, The University Press, Cambridge, 1897.

[3] H. Fripertinger, The cycle index of the symmetry group of the fullerene C_{60}, *MATCH Commun. Math. Comput. Chem.* **33** (1996) 121–138.

[4] S. Fujita, A simple method for enumeration of non-rigid isomers: An application of characteristic monomials, *Bull. Chem. Soc. Jpn.* **72** (1999) 2403–2407.

[5] S. Fujita, Characteristic monomials with chirality fittingness for combinatorial enumeration of isomers with chiral and achiral ligands, *J. Chem. Inf. Comput. Sci.* **4** (2000) 1101–1112.

[6] S. Fujita, *Combinatorial enumeration of graphs, three-dimensional structures, and chemical compounds*, Mathematical Chemistry Monographs: MCM 15, Kragujevac, 2013.
[7] S. Fujita, *Diagrammatical Approach to Molecular Symmetry and Enumeration of Stereoisomers*, Mathematical Chemistry Monographs: MCM 4, Kragujevac, 2007.
[8] S. Fujita, Inherent automorphism and Q-conjugacy character tables of finite groups: An application to combinatorial enumeration of isomers, *Bull. Chem. Soc. Jpn.* **71** (1998) 2309–2321.
[9] S. Fujita, Markaracter tables and Q-conjugacy character tables for cyclic groups: An application to combinatorial enumeration, *Bull. Chem. Soc. Jpn.* **71** (1998) 1587–1596.
[10] S. Fujita, Maturity of finite groups: An application to combinatorial enumeration of isomers, *Bull. Chem. Soc. Jpn.* **71** (1998) 2071–2080.
[11] S. Fujita, Mobius function and characteristic monomials for combinatorial enumeration, *Theor. Chem. Acc.* **101** (1999) 409–420.
[12] S. Fujita, Subduction of Q-conjugacy representations and characteristic monomials for combinatorial enumeration, *Theor. Chem. Acc.* **99** (1998) 224–230.
[13] S. Fujita, *Symmetry and Combinatorial Enumeration in Chemistry*, Springer-Verlag, Berlin-Heidelberg, 1991.
[14] S. Fujita, Systematic enumeration of ferrocene derivatives by unit-subduced-cycleindex method and characteristic-monomial method, *Bull. Chem. Soc. Jpn.* **72** (1999) 2409–2416.
[15] S. Fujita, *Combinatorial enumeration of graphs, three-dimensional structures, and chemical compounds*, Mathematical Chemistry Monographs: MCM 15, Kragujevac, 2013.
[16] M. Ghorbani, A. R. Ashrafi, Computing USCI table of an infinite family of fullerenes, *J. Comput. Theor. Nanosci.* **9** (2012) 681–687.
[17] S. Fujita, The unit-subduced-cycle-index methods and the characteristic-monomial method. Their relationship as group theoretical tools for chemical combinatorics, *J. Math. Chem.* **30**(3) (2001) 249–270.
[18] M. Ghorbani, A. R. Ashrafi, The cycle index of the symmetry group of fullerenes C_{24} and C_{150}, *Asian J. Chem.* **19**(2) (2007) 1109–1114.
[19] S. Hong, A. Dey, Network analysis of cosmic structures: network centrality and topological environment, Monthly Notices of the Royal Astronomical Society, **450**(2) (2015) 1999–2015.
[20] H. Shabani, A. R. Ashrafi, M. Ghorbani, Note on markaracter tables of finite groups, *SUT J. Math.* **52** (2016) 133–140.
[21] H. Shabani, A. R. Ashrafi, M. Ghorbani, Rational character table of some finite groups, *J. Algebr. Syst.* **3** (2016) 151–169.
[22] R. van de Weygaert et al., Alpha, Betti and the megaparsec universe: on the topology of thecosmic web, In Transactions on Computational Science XIV, *Lecture Notes in Computer Science, Springer 6970* (2011) 60–101.

Citation: M. Ghorbani, O. Ori, M. Putz, Eyes on the cosmic web: A tribute to Ali Reza Ashraf, J. Disc. Math. Appl. 8(4) (2023) 187–200.
https://doi.org/10.22061/jdma.2023.10093.1058